Polyurethane Composite Films Based on Modified Lignin and Reinforced with Silica Nanoparticles: Synthesis and Characterization

Bailiang Xue,[a,*] Yang Yang,[a] Rui Tang,[a] Yongchang Sun,[b] Shaoni Sun,[c] Xuefei Cao,[c] and Xinping Li [a,*]

Novel lignin-based polyurethane (LPU) and LPU-nanosilica composite films were prepared using *in situ* polymerization. The effects of various nanosilica contents on the structure and properties of the LPU matrix films were investigated by Fourier transform infrared spectroscopy (FTIR), scanning electron microscopy (SEM), energy dispersive spectroscopy (EDS), transmission electron microscopy (TEM), thermogravimetric analysis (TGA), dynamic thermomechanical analysis (DMA), tensile test, and contact angle measurements. The results showed that hydrogen bonding and cross-linking occurred between the -N-H and -C=O functional groups in the LPU-nanosilica films. Morphological and surface energy analyses showed uniform dispersion of amine modified silica nanoparticles in the LPU matrix at low concentrations. The incorporation of silica nanoparticles considerably improved the thermal stability and mechanical properties of the LPU films because of the introduction of silicon-oxygen bond between the LPU matrix and nanosilica. Overall, the introduction of small amounts of silica nanoparticles could improve the properties of the renewable LPU films, which are useful in the development of biomaterials.

Keywords: Lignin; Polyurethane; Nanosilica; Mechanical properties; Thermal stability

*Contact information: a: College of Bioresources Chemical and Materials Engineering, Shaanxi University of Science and Technology, Xi'an 710021, Shaanxi, China; b: Key Laboratory of Subsurface Hydrology and Ecological Effects in Arid Region, Ministry of Education, Chang'an University, Xi'an, China; c: Beijing Key Laboratory of Lignocellulosic Chemistry, Beijing Forestry University, Beijing, China; * Corresponding author: xuebailiang@sust.edu.cn*

INTRODUCTION

Lignin is one of the most abundant aromatic biopolymers, accounting for 18% to 35% of wood in nature. As a non-toxic, low-cost, and renewable resource, lignin is a substitute for some petrochemical products, which can alleviate the impact of the oil resource crisis and environmental pollution caused by non-biodegradable polymers. Currently, most lignin is utilized as a cheap fuel for power and heat in the pulp and paper mill, whereas only a small portion is employed for commercial uses, such as fillers, adhesives, surfactants, dispersants, coatings, *etc.* (Du *et al.* 2016; Huang *et al.* 2017; Wang *et al.* 2019). Therefore, there has been much effort to explore the value-added utilization of lignin.

Polyurethane (PU) is one of the most important and versatile class of polymeric plastics, which can be produced by polyaddition of diisocyanate or polyisocyanate and oligomeric hydroxyl polyol components (Pascault *et al.* 2002). Because most isocyanates and polyols are derived from fossil resources, it is crucial to seek renewable and sustainable resources for the partial or complete replacement of the petrochemical polyols in the

development of PU. Given that lignin is a renewable aromatic macro-polyol with abundant phenolic and aliphatic hydroxyl groups, lignin is a promising alternative for polyols in the production of PU (Li *et al.* 2016). In studies of the synthesis of lignin polyurethanes (LPUs), lignin is directly introduced into other polyols for the reaction with -NCO groups, which usually leads to phase separation due to the aggregation of lignin (Cateto *et al.* 2010; Chen *et al.* 2018). To improve the reactivity and compatibility between lignin and PU matrices, lignin modification reactions are performed using a suitable polyisocyanate, *via* etherification (Mahmood *et al.* 2015), esterification (Laurichesse *et al.* 2014), and liquefaction processes (Jin *et al.* 2011; Yona *et al.* 2014). However, the prepared LPU shows poor performance in terms of mechanical and thermal stability, which limits its commercialization.

Incorporating small amounts of nanoscale inorganic fillers into the LPU formulation can improve its mechanical, thermal, and thermo-mechanical properties. Inorganic/organic nanocomposites exhibit a good combination of properties between the inorganic nanoparticles and the organic polymer matrix due to the nanosize, higher surface and reactivity, and good adsorptive properties (Hu *et al.* 2014; Verdolotti *et al.* 2015; Yin *et al.* 2018). Silica nanoparticles as the inorganic nanoscale building blocks have attracted much attention due to their excellent physical and chemical properties, such as mild preparation conditions, large specific surface area, high surface activity, large adsorption capacity, and pore volume (Ghosh *et al.* 2011; Donato *et al.* 2012). To further improve the dispersion and surface activity of silica nanoparticles in the PU matrix, the surface of silica nanoparticles is modified with silane to increase the compatibility between the nanosilica and PU matrices (Liao *et al.* 2012). Seeni *et al.* (2014) found that castor oil based PU/nanosilica films modified with (3-aminopropyl)trimethoxysilane (APTMS) exhibit reduced surface energy and better mechanical and thermal properties. Kumar *et al.* (2015) reported that liquefied wood-based PU/nanosilica hybrid coatings hydrophobized by orthotrichlorosilane (OTS) showed better surface hardness and stability toward cold liquids. Furthermore, the surface of nanosilica has hydrophilic characteristics, which leads to a poor compatibility between the hydrophobic nanosilica and PU matrix. Lignin as an amphipathic substance could improve the hydrophobicity of nanosilica surface, enhancing their chemical interaction in LPU films. However, lignin-derived PU/nanosilica composites have not been studied.

In this work, industrial lignin was chosen as a starting material for preparing LPU films, and nanosilica particles were added to obtain LPU/nanosilica films with improved properties. LPU was prepared by the formation of the urethane structure using liquefied lignin at ambient temperature. Various amounts of nanosilica particles were incorporated into the reaction mixture. The obtained LPU-nanosilica films were analyzed by various physicochemical techniques to understand their structural, morphological, surface, thermal, and mechanical properties.

EXPERIMENTAL

Materials

Lignin in this study was kindly supplied by the Longlive Biological Technology Co. Ltd. (Shandong, China). The lignin was obtained from the corncob residue after hydrolysis of hemicelluloses. The chemical characteristics of the lignin were previously reported (Xue *et al.* 2014). The raw lignin contained 88.5% Klason lignin and 4.7% acid-

soluble lignin. (3-Aminopropyl) trimethoxysilane (APTMS) was purchased from Aladdin® (Shanghai, China). 4,4'-Diphenylmethane diisocyanate (MDI, 3.996 mmol/g) was provided by Adamas-beta® (Shanghai, China). Tetraethyl orthosilicate (TEOS), dibutyltin dilaurate (DBTDL), tetrahydrofuran (THF), glycerol, and polyethylene glycol with a molecular weight of 400 g/mol (PEG-400) were supplied by Damao Chemical Reagent Company (Tianjin, China). All chemicals were used as received.

Preparation of Amine Modification Nanosilica

Nanosilica was prepared as previously described, with slight modifications (Wang *et al.* 2011). Briefly, anhydrous ethanol (50 mL) and ammonia solution (3.5 mL) were mixed under constant stirring at room temperature (R.T.). Subsequently, TEOS (3.5 mL) was slowly added and then continuously stirred overnight at R.T. Afterwards, APTMS (0.7 mL) was added dropwise to the reaction with continuous stirring at R.T. for another 24 h. Finally, pure nanosilica was collected after several cycles of centrifugation and washing with anhydrous ethanol to remove the residual chemicals.

Preparation of LPU-nanosilica Films

Liquefied lignin-based polyols were prepared according to published work (Xue *et al.* 2015). A mixture of PEG-400 and glycerol (80:20; w/w) was used as the liquefying agent (solvent), where the ratio of lignin to solvents was kept at 1:5. Microwave heating was used for liquefaction at 140 ℃ for 5 min with 1.5% concentrated sulfuric acid (based on total mass of the mixture) as catalyst. The hydroxyl content of the liquefied lignin was determined by the method described in *ISO 14900:2017 Plastics -- Polyols for use in the production of polyurethane -- Determination of hydroxyl number*. The LPU-nanosilica films were prepared by a one-step method. The molar ratio of isocyanate to hydroxyl functional group (NCO/OH) was set to 1.0. Approximately 15 g of liquefied lignin and 0.3 g of DBTDL were dissolved in THF solution at 30 ℃ for 0.5 h. After MDI was added, the mixtures were stirred at 30 ℃ for 4 h. Various amounts of nanosilica (0.5%, 1%, 2%, 3%, based on the respective weight) were added to the reaction system for 0.5 h until everything appeared to be evenly dispersed. After the polymerization, the mixtures prepared in the previous section were immediately poured into a Teflon mold in air and allowed to cross-link in a ventilated oven at 30 ℃ for 24 h; then the LPU film was obtained. Each sample based on the content of nanosilica was referred as LPU-0.5%, LPU-1%, LPU-2%, and LPU-3%. A control sample without nanosilica was labeled as LPU-0. The NCO/OH ratio was calculated using Eq. 1,

$$\frac{[\mathrm{NCO}]}{[\mathrm{OH}]} = \frac{M_{\mathrm{MDI}} \times W_{\mathrm{MDI}}}{M_{\mathrm{polyol}} \times W_{\mathrm{polyol}}} \quad (1)$$

where M_{MDI} (9.028 mmol/g) is the content of the isocyanate group in MDI, M_{polyol} (8.628 mmol/g) is the content of the hydroxyl groups in the liquefied lignin based on our previous work (Xue *et al.* 2015), and W_{MDI} and W_{polyol} are the weights of MDI and liquefied lignin, respectively.

Characterization of LPU-nanosilica Films

The particle size distribution of synthesized nanosilica was measured using a Zetasizer Nano ZS (Malvern, UK). Fourier transform infrared (FTIR) spectra of the LPU-nanosilica films were recorded using a Bruker Vertex 70 (Billerica, MA) with a resolution

of 4 cm^{-1} over a scan of 400-4000 cm^{-1}. The ATR mode was used for testing. The morphology of the LPU-nanosilica films was determined using a field emission scanning electron microscope (SEM, S4800, Hitachi, Japan). The cross section obtained after quenching from liquid nitrogen was analyzed. The content of chemical elements was measured by EDS (EDAX, Ametek Materials Analysis Division, Mahwah, USA). High-resolution transmission electron microscopic (HR-TEM) images were obtained using a FEI Tecnai G2 F20 microscope (Hillsboro, OR, USA). TGA was performed using a NETZSCH STA449F3 (NETZSCH Scientific Instruments, Bavarian, Germany) under N_2 atmosphere with 50 mL/min with a heating rate of 10 °C/min. The viscoelasticity of the LPU-nanosilica films were analyzed in stretching mode using a DMA Q800 thermal analyzer (TA Instruments, New Castle, DE, USA). The measurements were performed in the temperature range from -60 °C to 110 °C with a frequency of 1.0 Hz and heating rate of 3.0 °C/min. The maximum dynamic force was 10 N. The dimension of the specimen used was 30 mm × 6 mm × 0.5 mm (length × width × thickness). The tensile test was conducted using a universal testing machine (AI-7000-NGD, Gotech Testing Machines Inc., Taizhong, China) at a cross-head speed of 10 mm/min with the thickness of 0.5 mm. The contact angles were recorded by the sessile drop method using OCA20 (Data Physics Corporation, San Jose, CA, USA). The measurements were repeated five times at different positions of each film. The surface energy of the LPU-nanosilica films was calculated by measuring the contact angles of distilled water and diiodomethane solvent with a test drop volume of 10 μL. The free surface energy was determined using two liquids with different polarity values, water (γ_L =72.80 mN/m, γ_L^d = 21.80 mN/m, γ_L^p = 51.00 mN/m) and diiodomethane (γ_L = 50.80 mN/m, γ_L^d = 50.80 mN/m, γ_L^p = 0.00 mN/m) (Tavares *et al.* 2018).

RESULTS AND DISCUSSION

Preparation of the LPU-nanosilica Films

As described in Fig. 1, the LPU-nanosilica films were prepared through a two-step process. In the first step, LPU was prepared by the formation of the urethane structure using liquefied lignin at ambient temperature. In the second step, the addition of various amounts of nanosilica introduced silicon-oxygen bonds to the LPU matrix, thereby obtaining the LPU-nanosilica films.

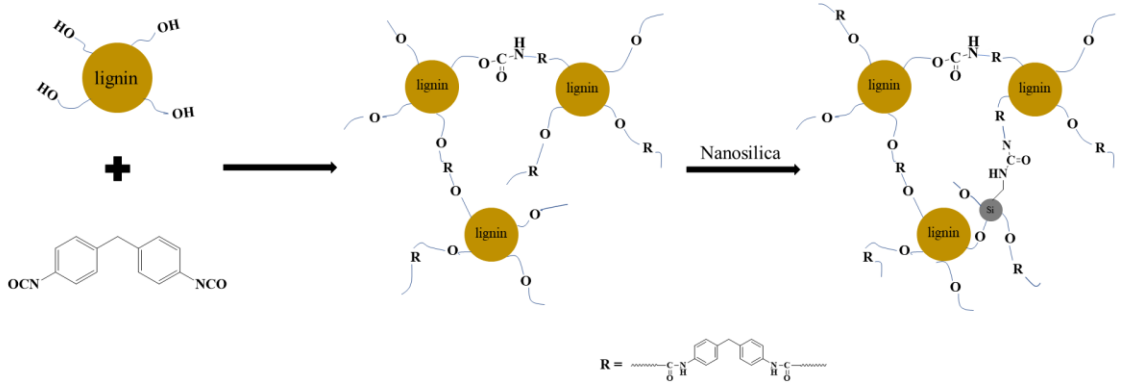

Fig. 1. Preparation of LPU-nanosilica films

The particle size distribution and SEM image of the prepared nanosilica is given in Fig. 2. The obtained nanosilica were homogeneous in size and spherical in shape, ranging from 37.84 nm to 91.82 nm. The chemical stability of nanosilica was improved by amine modification, which avoids self-condensation and agglomeration of nanosilica. The presence of amino groups also increases the activity of the nanosilica, which facilitates the subsequent reaction with LPU to introduce the silicon-oxygen bond (Kumar *et al.* 2012). To observe the dispersion of the silica nanoparticles in the LPU matrix, the sample LPU-2% was analyzed using HR-TEM. As shown in Fig. 3 well-defined dark circular spots were uniformly dispersed in the LPU matrix without the phenomenon of aggregates with 2% nanosilica content.

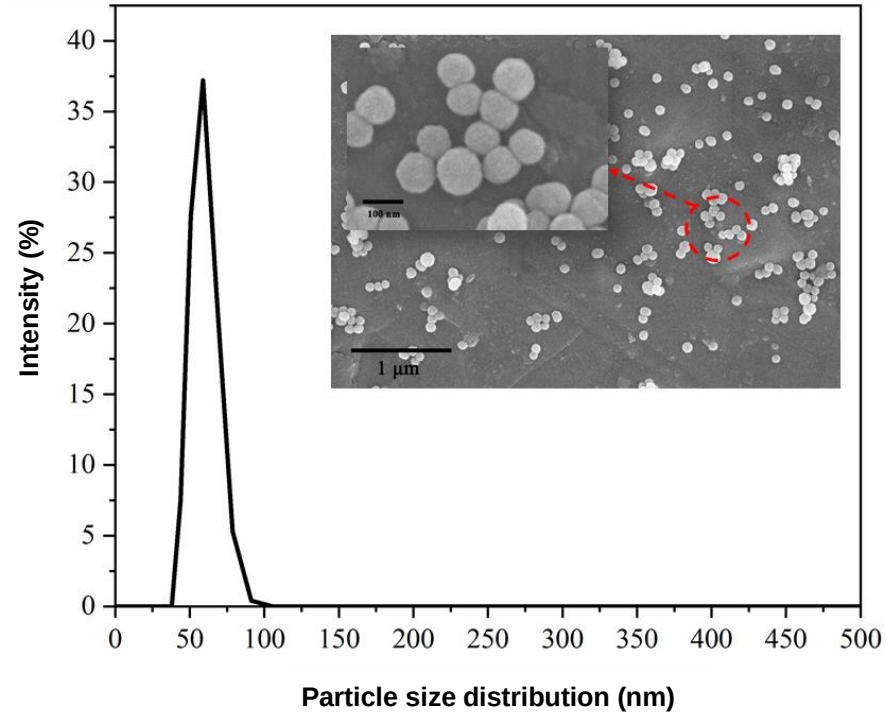

Fig. 2. Particle size distribution and SEM image of amine modification nanosilica

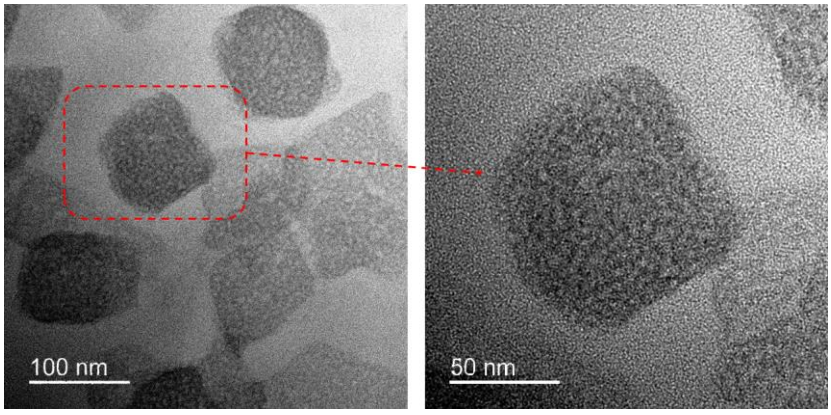

Fig. 3. HR-TEM images of LPU-2%

ATR-FTIR Spectra

The ATR-FTIR spectra of LPU-nanosilica films are shown in Fig. 4. The appearance of a broad absorption peak at 3294 cm^{-1} was attributed to -NH- groups. The peak at 2970 cm^{-1} was assigned to -OH groups in the cured LPU-nanosilica films. These results indicated that some unreacted hydroxyl groups remained in the films due to the steric hindrance in the liquefied lignin. The isocyanate also reacts with the amino group on the amine modification nanosilica. Furthermore, the peak around 2260 cm^{-1} to 2280 cm^{-1} due to the asymmetrical stretching vibration of the -NCO group was not observed, indicating that -NCO groups of the polyisocyanate components were almost completely reacted. These results confirmed the formation of the LPU-nanosilica films. Moreover, the peak at 1710 cm^{-1} belongs to the stretching vibration of the hydrogen-bonded carbonyl groups. In addition, the peaks at 1600 cm^{-1} and 1516 cm^{-1} were attributed to the skeletal vibration of the benzene ring of the lignin, and they did not change in the LPU-nanosilica films (Xue *et al.* 2015).

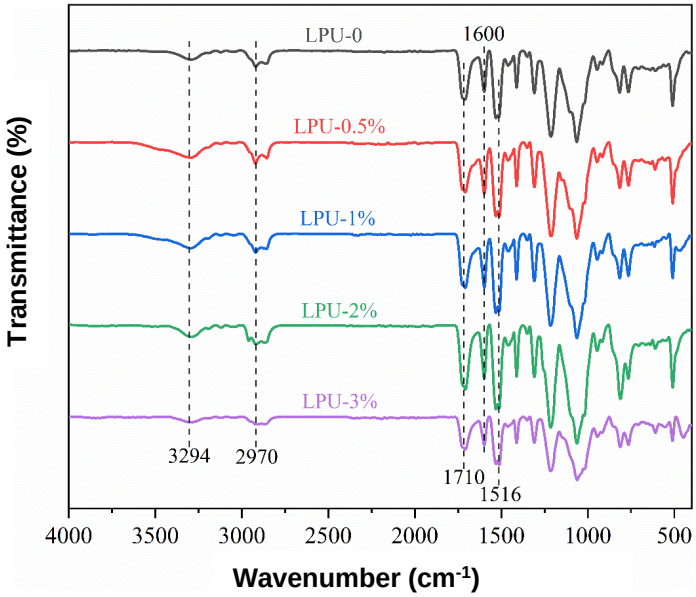

Fig. 4. ATR-FTIR spectra of LPU-nanosilica films

Morphology Analysis

The surface and cross sectional images of the LPU-nanosilica films are given in Fig. 5. Compared with the sample LPU-0 with smooth and flat morphology, the samples LPU-0.5% and LPU-3% showed the similar surface structures, suggesting that the silica nanoparticles did not affect the surface morphology of the LPU-nanosilica films. In the cross sectional images, the sample LPU-0 revealed a homogenous structure due to the cross-linked LPU. The introduction of amine modified silica nanoparticles in the LPU matrix displayed slight phase aggregation in the LPU matrix at the concentration of 0.5%. As the concentration of nanosilica was increased to 3% in the LPU matrix, the phase aggregation of their cross section became more apparent, which indicated agglomeration caused by high content of nanosilica. To analyze the content of nanosilica in the LPU-nanosilica films, the elemental compositions of LPU-nanosilica films were determined by EDS. The quantitative results of C, N, O, and Si elements are presented in Fig. 6. The elemental compositions of C, N, and O in the LPU-nanosilica films were almost

unchanged, except that the content of Si gradually increased from the sample LPU-0.5% with 4.10% Si to the LPU-1% with 7.22% Si, indicating that the silica nanoparticles were successfully introduced into the LPU matrix.

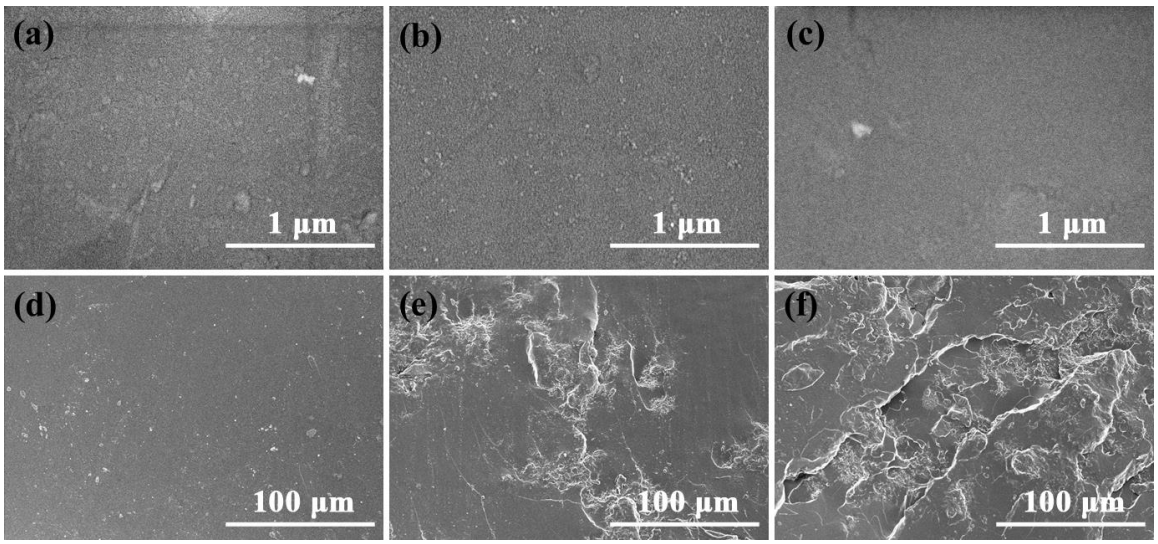

Fig. 5 SEM images of LPU-nanosilica films: (a-c) - surface images of LPU-0, LPU-0.5%, LPU-3%; and (d-f) - cross sectional images of LPU-0, LPU-0.5%, LPU-3%

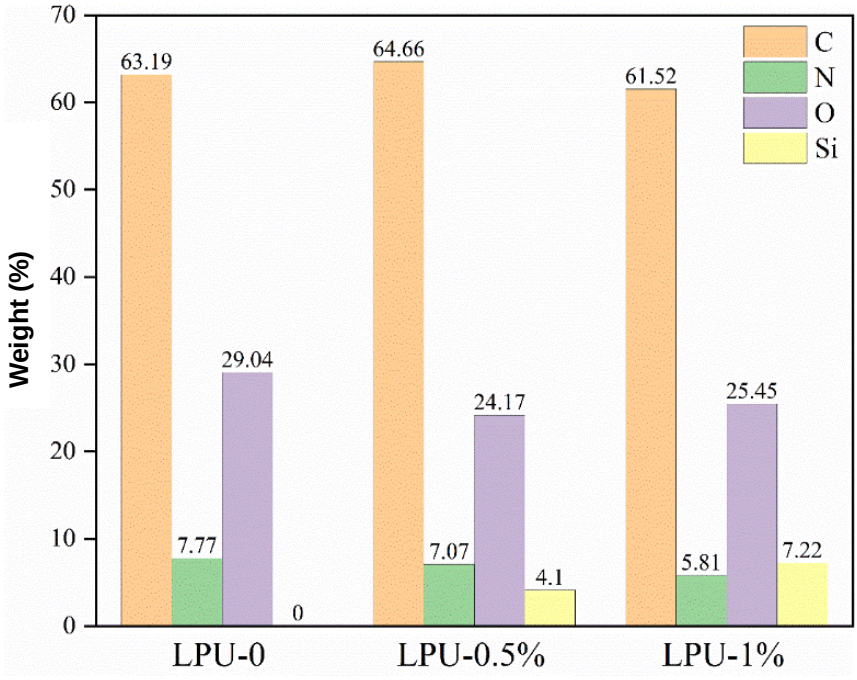

Fig. 6. EDS quantitative results for C, N, O, and Si (wt %) elements

Surface Energy

The change of surface energy can account for the dispersion of nanosilica in the LPU films. Contact angle measurements were obtained for the LPU-nanosilica films in

order to calculate their surface energy. The results are shown in Table 1. The surface energy was calculated using the Owens and Wendt equation (Owens and Wendt 1969),

$$\gamma_L (1 + \cos\theta) = 2 (\gamma_S^d \cdot \gamma_L^d)^{1/2} + 2 (\gamma_S^p \cdot \gamma_L^p)^{1/2} \quad (2)$$

where γ_L is the surface tension of the liquids, and γ_L^p, γ_L^d, γ_S^p, and γ_S^d are the surface tensions of the polar and dispersion components of the liquids and solids, respectively. The images of water droplets on LPU-nanosilica films are shown in Fig. 7. The contact angles of distilled water droplets on the samples LPU-0 and LPU-0.5% had the values of 74.5° and 77.5°, respectively. With the addition of nanosilica, the contact angle of LPU-nanosilica films gradually decreased. The lower contact angle may be the result of higher surface roughness with higher nanosilica loading although the assumed surface roughness was not clearly seen in the SEM analysis. The other possible reason was that the increased hydrophilic character of the surface may have been due to the presence of silanol groups of silica nanoparticles (Valles-Lluch *et al.* 2010). Surface energy of the LPU-nanosilica films increased with increasing addition of silica nanoparticles from 0.5% to 2%, and the surface energy of the sample LPU-2% was 47.25 mN/m. However, it is unexpected that the surface energy of the sample LPU-3% was only slightly reduced. This is probably because of the higher concentration of silica nanoparticles, which yielded a slightly agglomerated structure; leading to the reduced surface energy.

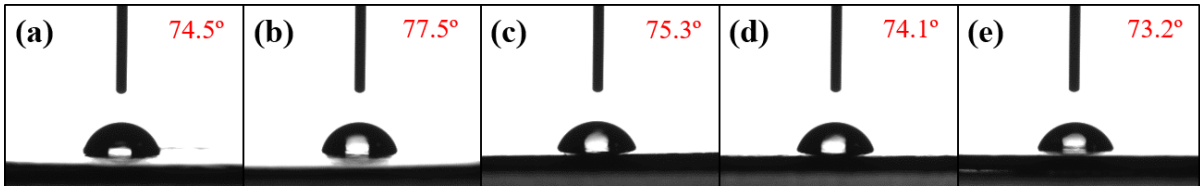

Fig. 7. Water droplets of LPU-nanosilica films: (a) LPU-0; (b) LPU-0.5%; (c) LPU-1%; (d) LPU-2%; and (e) LPU-3%

Table 1. Contact Angles and Surface Energies (γ_s), Dispersive (γ_s^d) and Polar (γ_s^p) Components of LPU-nanosilica Films

Samples	Static Contact Angle (θ°)		Surface Free Energy (mN/m)		
	Water	diiodomethane	γ_s^d	γ_s^p	γ_s
LPU-0	74.5	43.0	38.07	5.88	43.95
LPU-0.5%	77.5	40.0	39.61	4.35	43.96
LPU-1%	75.3	35.6	41.75	4.69	46.44
LPU-2%	74.1	34.6	42.21	5.04	47.25
LPU-3%	73.2	37.7	40.75	5.74	46.49

Thermogravimetric Studies

TGA measurements were taken to assess the thermal stability of the LPU-nanosilica films and are presented in Fig. 8. The LPU and LPU-nanosilica films showed similar weight loss pattern with accelerated temperature. The TGA indicated three main thermal degradation plateaus in the ranges of 100 to 800 °C. The first degradation step at 100 - 300 °C showed a 15% weight decrease in the LPU-nanosilica films, probably due to the vaporization of residual solvents and water. The second weight loss of approximately 60% mass loss in the range 300 to 500 °C was attributed to the breaking of carbon-carbon bonds between liquefied lignin and urethane linkages, primarily by the decomposition of urethane bonds with the elimination of carbon dioxide (Kurimoto *et al.* 2001; Wei *et al.* 2004).

Finally, the third degradation step at 500 to 800 ℃ was ascribed to the components through thermal degradation at elevated temperatures (Hubbe *et al.* 2018). The different thermal degradation temperatures and the residues for 600 ℃ were summarized in Table 2. Compared with the control LPU-0, the incorporation of nanosilica in the LPU matrix provided good thermal stability, which may be due to the introduction of silicon-oxygen bonds between the LPU matrix and nanosilica (Rahman and Padavettan 2012). This bond provided better reinforcement of thermal stability, which increasing the degradation temperature of the LPU-nanosilica films (Luo *et al.* 2012).

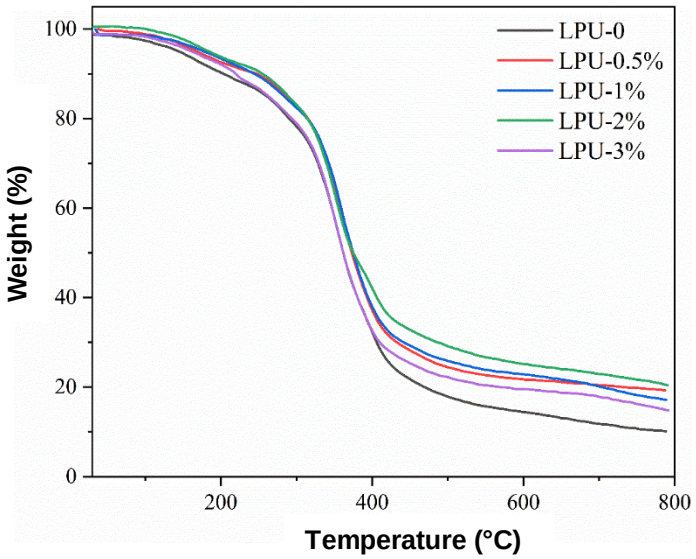

Fig. 8. TGA curves of LPU-nanosilica films

Table 2. Thermal Degradation Temperatures at 10% ($T_{10\%}$), 25% ($T_{25\%}$), and 50% ($T_{50\%}$) Mass Loss and Char Residue at 600 °C (R_{600}) for LPU-nanosilica Films

Samples	$T_{10\%}$ (°C)	$T_{25\%}$ (°C)	$T_{50\%}$ (°C)	R_{600} (%)
LPU-0	203.77	313.77	362.68	14.35
LPU-0.5%	252.08	330.56	373.92	21.93
LPU-1%	243.96	332.14	374.62	22.93
LPU-2%	255.94	331.08	376.06	25.46
LPU-3%	221.53	316.51	361.28	19.40

Mechanical Properties

Mechanical properties of LPU-nanosilica films are shown in Fig. 9 and Table 3. All films exhibited typical tensile properties of a non-crystalline polymer characterized by an initial elastic region, followed by a yield point and later undergoing plastic deformation. The tensile strength and Young's modulus of LPU-nanosilica films were significantly increased compared with sample LPU-0. This enhancement of tensile strength and Young's modulus was attributed to the presence of silica nanoparticles that hindered the segmental motion of the LPU chains through the introduction of silicon-oxygen bond between the silica nanoparticles and LPU matrix. More remarkably, the tensile strength and Young's modulus of the LPU-3% were inferior when compared to other LPU-nanosilica films. This was because the content of nanosilica was too high and the agglomeration affects the tensile strength and Young's modulus.

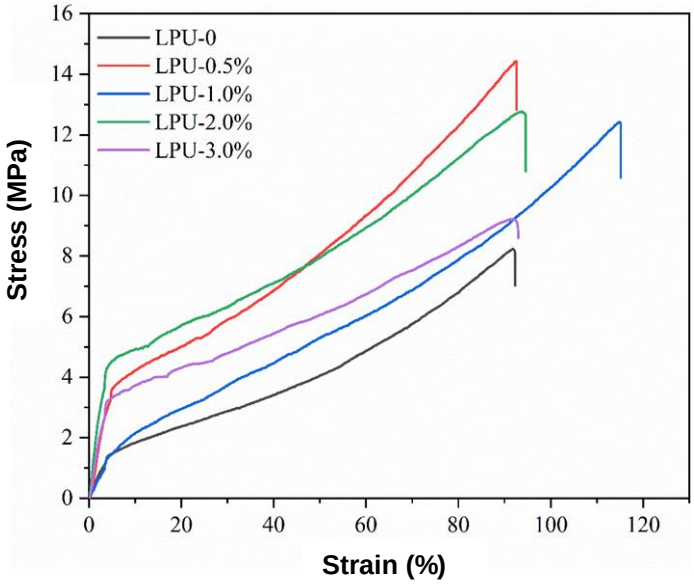

Fig. 9. Stress-strain curves of LPU-nanosilica films

Table 3. Mechanical Properties of LPU-nanosilica Films

Samples	Tensile Strength (MPa)	Young's Modulus (MPa)	Elongation at Break (%)
LPU-0	8.23 ± 0.79	34.62 ± 2.25	91.72 ± 2.31
LPU-0.5%	14.43 ± 0.76	72.49 ± 3.18	92.46 ± 2.63
LPU-1%	12.42 ± 0.78	32.35 ± 2.01	114.87 ± 2.11
LPU-2%	12.77 ± 0.81	108.55 ± 2.99	93.75 ± 2.59
LPU-3%	9.21 ± 0.73	83.91 ± 3.65	92.02 ± 2.41

Dynamic Thermomechanical Analysis

DMA experiments were conducted with samples LPU-0 and LPU-0.5% to examine the effect of nanosilica loading on the viscoelastic properties, and the results are presented in Fig. 10.

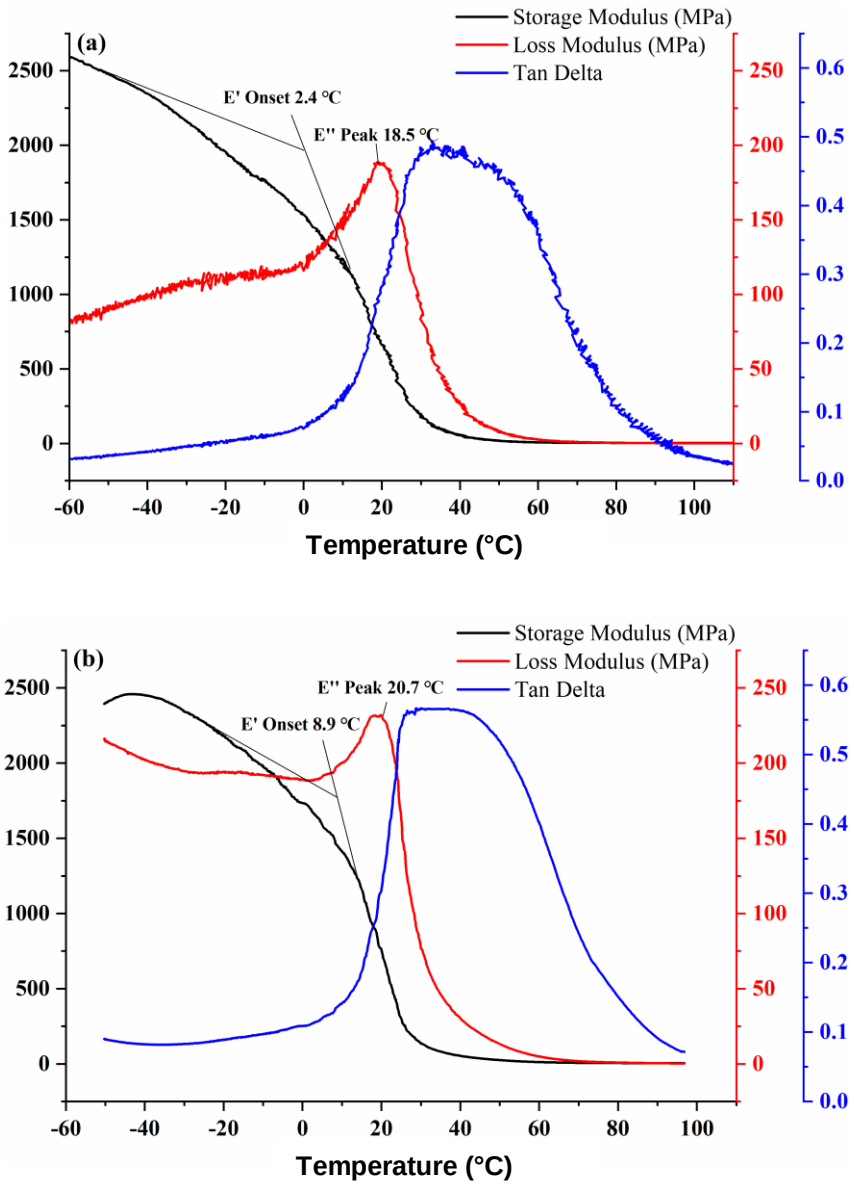

Fig. 10. DMA results of LPU-0 (a) and LPU-0.5% (b)

It can be seen that the LPU-0 had high storage modulus (*E'*) and stiffness at 2590 MPa, which indicated that LPU-nanosilica films have good mechanical properties via chemical crosslinking. In addition, the increase of the nanosilica content can affect the molecular chains movement and cause the increment of glass transition temperature and the onset of *E'* onset (the *E'* turning point). The *E'* onset transition temperature increased with the increasing nanosilica content, which illustrated the mechanical properties of the LPU-nanosilica films were improved by the addition of nanosilica. It showed that the *E'* of LPU-0.5% decreased more slowly than those of LPU-0 because of the presence of nanosilica, which restricted the mobility of LPU chains, thereby giving reinforcement to the LPU-nanosilica films.

CONCLUSIONS

1. Novel lignin-based polyurethanes (LPU)-nanosilica films were prepared using *in situ* polymerization.
2. The structure of LPU-nanosilica films was formed through cross-linking and hydrogen bonding.
3. Amine modification silica nanoparticles displayed uniform dispersion in the LPU matrix films at low concentrations.
4. The thermal stability and mechanical properties of LPU-nanosilica films were improved through the incorporation of nanosilica, which will broaden the practical utilizations of nanosilica reinforcement in the development of lignin-based materials.

ACKNOWLEDGEMENTS

The authors are grateful for the grants from the Natural Science Foundation of China (21706154, 41702367), National Key Research and Development Program of China (2017YFB0307903), Natural Science Foundation of Shaanxi Province, China (2019JQ-277) and the Doctoral Scientific Research Fund by Shaanxi University of Science & Technology (BJ15-26).

REFERENCES CITED

Cateto, C. A., Barreiro, M. F., Rodrigues, A. E., Brochier-Salon, M. C., Thielemans, W., and Belgacem, M. N. (2010). "Lignins as macromonomers for polyurethane synthesis: A comparative study on hydroxyl group determination," *J. Appl. Polym. Sci.* 109(5), 3008-3017. DOI: 10.1002/app.28393

Chen, C., Li, F., Zhang, Y., Wang, B., Fan, Y., Wang, X., and Sun, R. (2018). "Compressive, ultralight and fire-resistant lignin-modified graphene aerogels as recyclable absorbents for oil and organic solvents," *Chem. Eng. J.* 350, 173-180. DOI: 10.1016/j.cej.2018.05.189

Donato, R. K., Donato, K. Z., Schrekker, H. S., and Matejka, L. (2012). "Tunable reinforcement of epoxy-silica nanocomposites with ionic liquids," *J. Mater. Chem.* 22(19), 9939-9948. DOI: 10.1039/c2jm30830d

Du, X. Y., Lucia, L. A., and Ghiladi, R. A. (2016). "Development of a highly efficient pretreatment sequence for the enzymatic saccharification of loblolly pine wood," *ACS Sustain. Chem. Eng.* 4(7), 3669-3678. DOI: 10.1021/acssuschemeng.6b00198

Ghosh, S., Maity, S., and Jana, T. (2011). "Polybenzimidazole/silica nanocomposites: Organic-inorganic hybrid membranes for PEM fuel cell," *J. Mater. Chem.* 21(38), 14897-14906. DOI: 10.1039/c1jm12169c

Hu, Z., and Donato, G. (2014). "Novel nanocomposite hydrogels consisting of layered double hydroxide with ultrahigh tensibility and hierarchical porous structure at low inorganic content," *Adv. Mater.* 26(34), 5950–5956. DOI: 10.1002/adma.201400179

Huang, C. X., He, J., Narron, R., Wang, Y. H., and Yong, Q. (2017). "Characterization of kraft lignin fractions obtained by sequential ultrafiltration and their potential

application as a biobased component in blends with polyethylene," *ACS Sustain. Chem. Eng.* 5(12), 11770-11779. DOI: 10.1021/acssuschemeng.7b03415

Hubbe, M. A., Pizzi A., Zhang, H., and Halis, R. (2018). "Critical links governing performance of self-binding and natural binders for hot-pressed reconstituted lignocellulosic board without added formaldehyde: A review," *BioResources* 13(1), 2049-2115. DOI: 10.15376/biores.13.1.Hubbe

Jin, Y. Q., Ruan, X. M., Cheng, X. S., and Lü, Q. F. (2011). "Liquefaction of lignin by polyethyleneglycol and glycerol," *Bioresource Technol*. 102(3), 3581-3583. DOI: 10.1016/j.biortech.2010.10.050

Jung, H. S., Moon, D. S., and Lee, J. K. (2012). "Quantitative analysis and efficient surface modification of silica nanoparticles," *J. Nanomater*. 2012(11), 2817-2827. DOI: 10.1155/2012/593471

Kumar, A., Petrič, M., Kričej, B., Žigon, J., Tywoniak, J., Hajek, P., Škapin, A. S., and Pavlič, M. (2015). "Liquefied-wood-based polyurethane–nanosilica hybrid coatings and hydrophobization by self-assembled monolayers of orthotrichlorosilane (OTS)," *ACS Sustain. Chem. Eng.* 3(10), 2533-2541. DOI: 10.1021/acssuschemeng.5b00723

Kurimoto, Y., Takeda, M., Doi, S., Tamura, Y., and Ono, H. (2001). "Network structures and thermal properties of polyurethane films prepared from liquefied wood," *Bioresource Technol. 77*(1), 33-40. DOI: 10.1016/S0960-8524(00)00136-X

Laurichesse, S., Huillet, C., and Averous, L. (2014). "Original polyols based on organosolv lignin and fatty acids: New bio-based building blocks for segmented polyurethane synthesis," *Green Chem.* 16(8), 3958-3970. DOI: 10.1039/c4gc00596a

Li, M. F., Yang, S., and Sun, R. C. (2016). "Recent advances in alcohol and organic acid fractionation of lignocellulosic biomass," *Bioresource Technol.* 200, 971-980. DOI: 10.1016/j.biortech.2015.10.004

Liao, Y. C., Wu, X. F., Wang, Z., Yue, R. L., Liu, G. and Chen, Y. F. (2012). "Composite thin film of silica hollow spheres and waterborne polyurethane: Excellent thermal insulation and light transmission performances," *Mater. Chem. Phys.* 133, 642-648. DOI: 10.1016/j.matchemphys.2012.01.041

Luo, Z., Hong, R. Y., Xie, H. D., and Feng, W. G. (2012). "One-step synthesis of functional silica nanoparticles for reinforcement of polyurethane coatings," *Powder Technol.* 218, 23-30. DOI: 10.1016/j.powtec.2011.11.023

Mahmood, N., Yuan, Z. S., Schmidt, J., and Xu, C. B. (2015). "Preparation of bio-based rigid polyurethane foam using hydrolytically depolymerized kraft lignin via direct replacement or oxypropylation," *Eur. Polym. J.* 68, 1-9. DOI: 10.1016/j.eurpolymj.2015.04.030

Owens, D. K., and Wendt, R. C. (1969). "Estimation of the surface free energy of polymers," *J. Appl. Polym. Sci.* 13(8), 1741-1747. DOI: 10.1002/app.1969.070130815

Pascault, J. P., Sautereau, H., Verdu, J., and Williams, R. J. J. (2002). "Glass transition and transformation diagrams in thermosetting polymers," *Thermoseting Polymers*, New York, p. 4.

Rahman, I. A., and Padavettan, V. (2012). "Synthesis of silica nanoparticles by sol-gel: Size-dependent properties, surface modification, and applications in silica-polymer nanocomposites — A review," *J. Nanomater* 2012, 15. DOI: 10.1155/2012/132424

Seeni Meera, K. M., Murali Sankar, R., Paul, J., Jaisankar, S. N., and Mandal, A. B. (2014). "The influence of applied silica nanoparticles on a bio-renewable castor oil based polyurethane nanocomposite and its physicochemical properties," *Phys. Chem. Chem. Phys.* 16(20), 9276-9288. DOI: 10.1039/C4CP00516C

Tavares, L. B., Ito, N. M., Salvadori, M. C., dos Santos, D. J. and Rosa, D. S. (2018). "PBAT/kraft lignin blend in flexible laminated food packaging: Peeling resistance and thermal degradability," *Polym. Test.* 67, 169-176. DOI: 10.1016/j.polymertesting.2018.03.004

Valles-Lluch, A., Ferrer, G. G., and Pradas, M. M. (2010). "Effect of the silica content on the physico-chemical and relaxation properties of hybrid polymer/silica nanocomposites of P(EMA-co-HEA)," *Eur. Polym. J.* 46(5), 910-917. DOI: 10.1016/j.eurpolymj.2010.02.004

Verdolotti, L., Lavorgna, M., Lamanna, R., Di Maio, E., and Iannace, S. (2015). "Polyurethane-silica hybrid foam by sol–gel approach: Chemical and functional properties," *Polymer* 56, 20-28. DOI: 10.1016/j.polymer.2014.10.017

Wang, W. L., Wang, M., Huang, J. L., Zhao, X. J., Su, Y. H., Wang, Y. Q., and Li, X. P. (2019). "Formate-assisted analytical pyrolysis of kraft lignin to phenols," *Bioresource Technol.* 278, 464-467. DOI: 10.1016/j.biortech.2019.01.078

Wang, Z. K., Wang, D., Wang, H., Yan, J. J., You, Y. Z., and Wang, Z. G. (2011). "Preparation of biocompatible nanocapsules with temperature-responsive and bioreducible properties," *J. Mater. Chem.* 21(40), 15950-15956. DOI: 10.1039/c1jm12570b

Wei, Y., Cheng, F., Li, H. and Yu, J. (2004). "Synthesis and properties of polyurethane resins based on liquefied wood," *J. Appl. Polym. Sci.* 92, 351-356. DOI: 10.1002/app.20023

Xue, B. L., Wen, J. L., and Sun, R. C. (2014). "Lignin-based rigid polyurethane foam reinforced with pulp fiber: Synthesis and characterization," *ACS Sustain. Chem. Eng.* 2(6), 1474-1480. DOI: 10.1021/sc5001226

Xue, B. L., Wen, J. L., and Sun, R. C. (2015). "Producing lignin-based polyols through microwave-assisted liquefaction for rigid polyurethane foam production," *Materials* 8(2), 586-599. DOI: 10.3390/ma8020586

Yin, Y. Y., Lou, C. Q., Hubbe, M. A., Tian, X. Z., Jiang, X., Wang, H. B., and Gao, W. D. (2018). "Synergy of silane and polyacrylate treatments to prepare thermally stable and hydrophobic cellulose nanocrystals," *Chem. Lett.* 47, 1272-1275. DOI: 10.1246/cl.180559

Yona, A. M. C., Budija, F., Kricej, B., Kutnar, A., Pavlic, M., Pori, P., Tavzes, C., and Petric, M. (2014). "Production of biomaterials from cork: Liquefaction in polyhydric alcohols at moderate temperatures," *Ind. Crop. Prod.* 54, 296-301. DOI: 10.1016/j.indcrop.2014.01.027

Article submitted: March 8, 2019; Peer-review completed: May 3, 2019; Revised version received: June 4, 2019; Accepted: June 5, 2019; Published: June 13, 2019.
DOI: 10.15376/biores.14.3.6100-6113